Journal of Catalysis **209,** 445–455 (2002)
doi:10.1006/jcat.2002.3648

The Preparation, Characterization, and Catalytic Behavior of MoVTeNbO Catalysts Prepared by Hydrothermal Synthesis

P. Botella, J. M. López Nieto,[1] B. Solsona, A. Mifsud, and F. Márquez

Instituto de Tecnología Química, UPV-CSIC, Avenida de los Naranjos s/n, 46022-Valencia, Spain

Received December 21, 2001; revised April 10, 2002; accepted April 16, 2002

MoVTeNbO catalysts with several Mo/Te/V/Nb (1/0.15–0.7/0–0.5/0–0.9) contents have been prepared by hydrothermal synthesis and tested in the selective oxidation of propane and propene to acrylic acid. Characterization results (XRD, FTIR, SEM–EDX, and XPS) and catalytic tests show important differences, depending on the composition of the catalysts. In this way, several crystalline phases have been observed in the active and selective catalysts, i.e., $TeMo_5O_{16}$, $(Mo_{0.93}V_{0.07})_5O_{14}$, $3MoO_2Nb_2O_5$, and/or $Nb_{0.09}Mo_{0.91}O_{2.80}$, and a new TeVMo oxide crystalline phase. Vanadium is the key element in the activation of propane and the selective achievement of acrylic acid while V- and/or Nb-doped MoTe-containing crystalline phases are related to the selective transformation of propene to acrolein/acrylic acid. However, the role of Nb ions is still unclear. Nb-containing MoVTe catalysts present both high activity and high selectivity to acrylic acid. Space time yields of acrylic acid closer than 70 and 600 $g_{AA}\ Kg^{-1}_{cat}\ h^{-1}$ can be obtained at 380°C during the oxidation of propane (keeping selectivities of about 55%) and propene (keeping selectivities of about 80%), respectively.

Key Words: **oxidation of propane and propene; acrylic acid; acrolein; acrylonitrile; Mo-V-Te-Nb oxide catalysts; hydrothermal synthesis; X-ray diffraction; FTIR; SEM–EDX; XPS.**

INTRODUCTION

Mo–V–Te–Nb mixed metal oxides have recently been proposed as active and selective catalysts in the oxidation of propane to acrylic acid (1–5) and yields of acrylic acid of 45% have been reported in the patent literature (1–3). These catalysts are similar to those reported for the ammoxidation of propane to acrylonitrile (6–10).

The nature of the active and selective sites in the MoVTeNbO catalysts is still under discussion. Although, at first, the catalytic results for the ammoxidation of propane were thought to be related to the presence of a single-crystalline phase (1), they were later associated with the formation of two major phases, denoted M1 and M2 (7, 8). The catalytic behavior of MoVTeNb catalysts in the oxidation of propane to acrylic acid could also be explained by the presence of three moieties (11): (i) a V–Nb–O phase as paraffin activator; (ii) a Te–Mo–O phase to oxidize olefins to aldehyde; and (iii) a V–Mo–O phase to convert the aldehyde to the corresponding acid. XRD patterns of the catalysts selective for both the ammoxidation (10) and the oxidation of propane to acrylic acid (5) suggest the presence of more than two crystalline phases, although the nature and the role of each one is still unclear.

The M1 and M2 phases in multicomponent MoVTeNbO catalysts have been proposed to correspond to $Te_{0.33}MO_3$ and $Te_{0.2}MO_{3.2}$ (with $M =$ Mo, V, and Nb) stoichiometries, respectively (12). However, no catalytic results were presented.

Recently, new MoVTeO and MoVTeNbO crystalline phases, isomorphous with $Sb_4Mo_{10}O_{31}$ and probably related to $Te_{0.33}MO_3$ (13), have been reported to be inactive in propane oxidation but active and selective in the oxidation of propene to acrolein and acrylic acid. So, the other crystalline phases, i.e. MoVO and/or MoNbO oxides, must be present in MoVTeNb to activate propane. On the other hand, their catalytic performances strongly depend on both the chemical composition and the catalyst preparation procedure (1–17). Watanabe and Koyasu (9) compared several methods of preparing MoVNbTe mixed oxides catalysts for the ammoxidation of propane. They observed that materials prepared hydrothermally gave catalyst precursors, which showed twice the activity after calcination than those prepared by the dry-up method. In this way, Ueda and co-workers (15, 16) reported that catalysts for the selective oxidation of propane to acrylic acid could be obtained by hydrothermal synthesis. They reported the synthesis of a $Mo_6V_3Te_1O_x$ catalyst relatively selective in the oxidation of propane to acrylic acid, although the yield of acrylic acid was lower than those reported in the patent literature.

Recently, it has been reported that the use of hydrothermal synthesis can help to develop most active and selective MoVNbTeO catalysts for the oxidation of propane to acrylic acid (5). In this paper we report the preparation and characterization of MoVTeNb mixed oxides catalysts, prepared by hydrothermal synthesis, and the influence of the catalyst composition on the catalytic behavior in the oxidation of propane and propene to acrylic acid.

[1] To whom correspondence should be addressed. Fax: 34-96-3877809. E-mail: jmlopez@itq.upv.es.

0021-9517/02 $35.00

EXPERIMENTAL

Catalyst Preparation

MoVTeNb mixed oxides catalysts were prepared by a hydrothermal method, using vanadyl sulfate, niobium oxalate, ammonium hexamolybdotellurate, $(NH_4)_6TeMo_6O_{24} \cdot nH_2O$, and water with different Mo/V/Te/Nb atomic ratios (5). The gels were autoclaved in teflon-lined stainless-steel autoclaves at 175°C for 48 h. The resulting precursors were filtered, washed, dried at 80°C for 16 h, and calcined at 600°C for 2 h in a N_2 stream. The compositions of both the synthesis gel and the corresponding calcined samples are presented in Table 1.

Catalyst Characterization

BET specific surface areas were measured on a Micromeritics ASAP 2000 instrument (adsorption of krypton) and on a Micromeritics Flowsorb (adsorption of N_2).

X-ray diffraction patterns (XRD) were collected using a Philips X'Pert diffractometer equipped with a graphite monochromator, operating at 40 kV and 45 mA, and employing nickel-filtered Cu$K\alpha$ radiation ($\lambda = 0.1542$ nm).

The infrared spectra were recorded at room temperature on a NICOLET 710 FTIR spectrometer equipped with a Data Station. Dried samples (20 mg) were mixed with 100 mg of dry KBr and pressed into a disk (600 kg cm^{-2}).

Scanning electron microscopy (SEM) and EDX microanalyses were performed on a JEOL JSM 6300 LINK ISIS instrument. The quantitative EDX analysis was performed using an Oxford LINK ISIS System with the SEMQUANT program, which introduces the ZAF correction.

Photoelectron spectra (XPS) were recorded on a VG-Escalab-210 electron spectrometer using Mg$K\alpha$ radiation (Mg$K\alpha = 1253.6$ eV) of a twin anode in the constant analyzer energy mode, with a pass energy of 50 eV. To facilitate the analysis of the catalysts we obtained self-supporting wafers 13 mm in diameter that were fixed on a sample holder. Samples were previously outgassed at 100°C for 2 h in the preparation chamber of the spectrometer and subsequently transferred to the analysis chamber. The pressure of the main chamber was maintained at 5×10^{-10} mB. The binding energy (BE) scale was regulated by setting the C 1s transition at 284.6 eV. The accuracy of the BE was ±0.1 eV.

Catalytic Tests

The catalytic experiments were carried out in a fixed-bed quartz tubular reactor (i.d., 12 mm; length, 400 mm), working at atmospheric pressure (5). Catalyst samples (0.3- to 0.5-mm particle size) were introduced into the reactor and diluted with 2–4 g of silicon carbide (0.5- to 0.75-mm particle size) in order to keep a constant volume in the catalyst bed. The flow rate and the amount of catalyst were varied (from 25 to 100 cm^3 min^{-1} and from 0.3 to 3.0 g, respectively) in order to achieve different propane conversion levels. The feed consisted of a mixture of propane/oxygen/water/helium with a molar ratio of 4/8/30/58. Experiments were carried out in the 350–420°C temperature interval in order to achieve the highest selectivity to partial oxidation products.

RESULTS AND DISCUSSION

Table 1 shows some characteristics of the calcined samples. The surface area of the catalysts depends on the catalyst composition. In general, the incorporation of Nb increases the surface area, which could be explained by the presence of oxalic acid during the preparation of Nb-containing catalysts (5).

The chemical composition of calcined samples strongly depends on the amount of each element incorporated into the synthesis gel. In this way, it can be noticed that the higher the vanadium amount in the synthesis gel, the higher the vanadium and the lower the tellurium contents in the calcined materials. An opposite trend in the vanadium and tellurium contents in the solids is observed when the concentration of Te in the synthesis gel increases. However, an influence of the Nb-content on the incorporation of other

TABLE 1

Characteristics of MoVTeNbO Catalysts

Sample	S_{BET} (m^2 g^{-1})	Mo/Te/V/Nb			
		Gel composition[a]	Bulk composition[a]	EDX composition	XPS composition
Cat-1	1.0	1/0.17/0/0.12	1/0.69/0/0.86	nd[b]	1/0.45/0/0.51
Cat-2	3.5	1/0.17/0.12/0.12	1/0.42/0.14/0.16	nd	1/0.33/0.09/0.47
Cat-3	9.1	1/0.17/0.36/0.12	1/0.23/0.22/0.15	1:0.23:0.11:0.22	1/0.19/0.11/0.20
Cat-4	14.3	1/0.17/0.45/0.12	1/0.17/0.26/0.18	nd	nd
Cat-5	11.8	1/0.17/0.73/0.12	1/0.16/0.34/0.17	1/0.14/0.36/0.23	1/0.16/0.31/0.17
Cat-6	6.4	1/0.17/0.36/0	1/0.19/0.15/0	1/0.14/0.14/0	1/0.11/0.20/0
Cat-7	10.1	1/0.17/0.36/0.24	1/0.17/0.15/0.43	1/0.16/0.15/0.50	1/0.22/0.06/0.37

[a] Chemical composition has been done by atomic absorption spectroscopy.
[b] nd, Not determined.

elements is not clear, although the higher the Nb content in gel, the higher its incorporation into the solid.

XRD Study

Figure 1 shows the XRD patterns of calcined MoVTeNb catalysts prepared hydrothermally. The sample without vanadium shows the presence of $Nb_{0.09}Mo_{0.91}O_{2.80}$ [JCPDS, 27-1310] and $3MoO_2Nb_2O_5$ [JCPDS, 18-840] (Fig. 1a), while no Te-containing crystalline phase was detected.

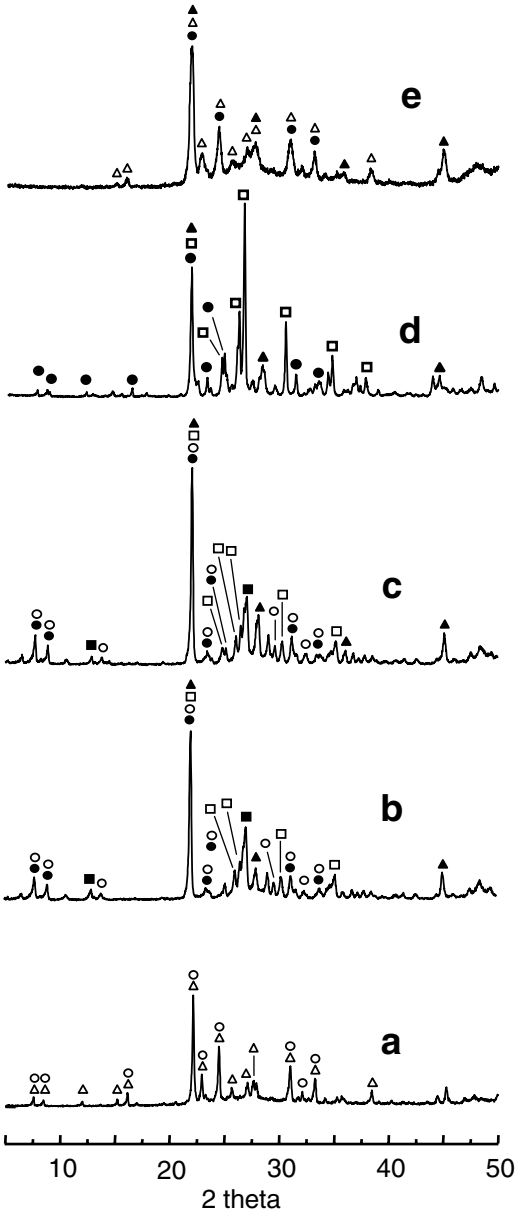

FIG. 1. XRD pattern of V- and/or Nb-containing MoTe samples after calcination at 600°C for 2 h: (a) Cat-1; (b) Cat-3; (c) Cat-5; (d) Cat-6; and (e) Cat-7. Symbols: (●) $(Mo_{0.93}V_{0.07})_5O_{14}$; (○) $Nb_{0.09}Mo_{0.91}O_{2.80}$; (■) MoO_3; (□) $TeMo_5O_{16}$; (△) $3MoO_2 \cdot Nb_2O_5$; and (▲) TeMO (TeVMoO and/or TeVNbMoO) crystalline phase (13).

The incorporation of vanadium provokes the appearance of peaks at $2\theta = 8.7$, 21.7, 24.6, 26.2, 26.6, 30.5, 34.4, and 34.9°, which suggests the presence of $TeMo_5O_{16}$ [JCPDS, 31-874] and/or $TeMo_4O_{13}$ [JCPDS, 34-622], while the appearance of peaks at $2\theta = 7.7$, 8.7, 14.0, 22.1, 23.3, 24.9, 29.7, 31.5, 32.4, and 33.5 could be related to the presence of $(Mo_{0.93}V_{0.07})_5O_{14}$ [JCPDS, 31-1437] and/or $Nb_{0.09}Mo_{0.91}O_{2.80}$ (Figs. 1b and 1c). Finally, the peaks at $2\theta = 22.1$, 28.2, 36.2, 44.7, and 50.0 (Figs. 1b and 1c) can be assigned to a new TeVMoO or TeVNbMoO (TeMO; M = Mo, V, and Nb) crystalline phase (13), which could correspond to the phase M1 ($Te_{0.33}MO_3$; M = Mo, V, and Nb) proposed by Aouine *et al.* (12).

The last XRD patterns of MoVTeNb catalysts are relatively different from those previously reported by Ushikubo *et al.* (7) but similar to those recently reported by our group (5) and by Asakura *et al.* (10). Although the peak at $2\theta = 22.1°$ can be related to the presence of several Mo-containing phases, i.e., $TeMo_5O_{16}$, $TeMo_4O_{13}$, $(Mo_{0.93}V_{0.07})_5O_{14}$, and $Nb_{0.09}Mo_{0.91}O_{2.80}$ (~3.9–4.0 Å d-spacing), the peak at $2\theta = 28.2°$ is the most important reflection of the new TeMO crystalline phases (13). So, the intensity ratio between the peaks at $2\theta = 22.1$ and 28.2° ($I_{22.1}/I_{28.2}$) can be used, in a first approach, to estimate the relative concentration of the new TeMO crystalline phase. Accordingly, the XRD pattern reported here shows a relative concentration of the TeVMoO and/or TeVNbMoO crystalline phase lower than that reported in Refs. (7, 12). Furthermore, at high V contents, the intensities of the most important peaks of $(Mo_{0.93}V_{0.07})_5O_{14}$ and the new TeMO phases increase with the V content (Fig. 1c).

On the other hand, the XRD pattern of the Nb-free sample shows the presence of $TeMo_5O_{16}$ (the most intense peaks), $(Mo_{0.93}V_{0.07})_5O_{14}$, and Te$M$O (Fig. 1d). The incorporation of Nb provokes a decrease in the intensities of the peaks corresponding to $TeMo_5O_{16}$ and the appearance of peaks at $2\theta = 7.7, 8.7, 14.0, 22.1, 23.3, 24.9, 29.7, 31.5, 32.4$, and 33.5°, corresponding to $Nb_{0.09}Mo_{0.91}O_{2.80}$ (Fig. 1b). However, an increase in Nb content in the catalyst favors the development of enriched Nb phases like $3MoO_2Nb_2O_5$ (peaks at $2\theta = 15.4$, 16.3, 22.2, 23.1, 24.6, 25.9, 27.2, 27.8, 31.2, 33.4, and 38.6°) (Fig. 1e).

FT-IR Results

Figure 2 shows the FT-IR spectra of samples with different V and/or Nb contents. The sample without vanadium presents three bands in the low-wavenumber region: a broad band in the 920- to 860-cm^{-1} range and two bands at 751 and 608 cm^{-1} (Fig. 2a) related to the symmetric stretching vibration of the Mo=O group (bands at 900–1000 cm^{-1}) and to antisymmetric vibrations of Mo–O–Me (Me = Mo, Nb, Te) bridging bonds (bands at 700–900 cm^{-1}) (18, 19), which are shifted to higher wavenumber (884, 792, and 640 cm^{-1}, respectively) by the incorporation of V atoms.

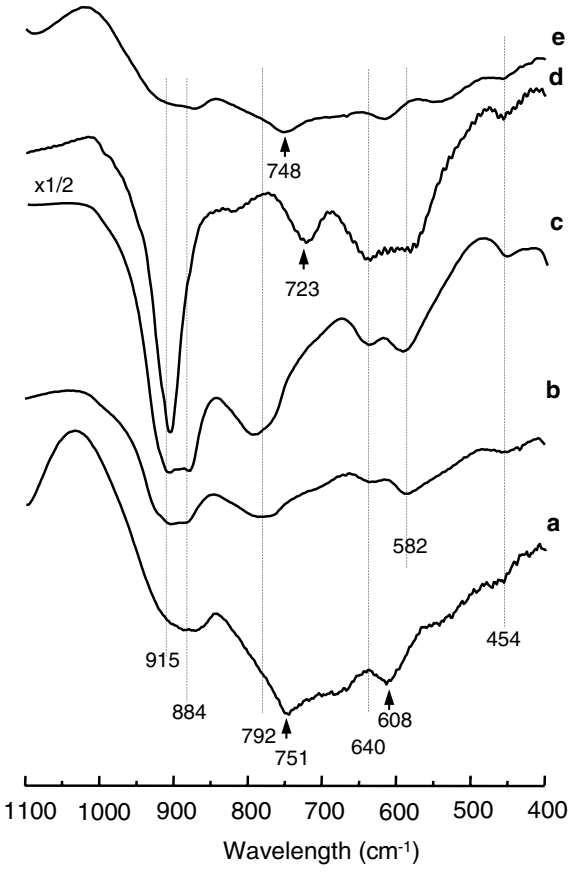

FIG. 2. IR spectra of V- and/or Nb-containing MoTe samples after calcination at 600°C for 2 h: (a) Cat-1; (b) Cat-3; (c) Cat-5; (d) Cat-6; and (e) Cat-7.

In addition, new bands at ca. 915, 582, and 454 cm^{-1}, probably related to a V=O group and V–O–Me bonds, are also observed (Fig. 2, spectra b and c).

The FT-IR spectrum of the Nb-free sample shows the presence of bands at ca. 905, 723, 640, 582, and 454 cm^{-1} (Fig. 2d), which according to XRD results should be related to the presence of $TeMo_5O_{16}$ or $TeMo_4O_{13}$ phases. The IR spectrum of $TeMo_5O_{16}$ is characterized by the presence of bands at ca. 913, 800, 765, 630, 725, 540, and 500 cm^{-1} (18), whereas the IR spectrum of $TeMo_4O_{13}$ presents a Mo=O stretching frequency at 930 cm^{-1} (low-temperature α'-$TeMo_4O_{13}$), or a more complex bond structure with $\nu_{Mo=O}$ at 928 and 952 cm^{-1} with two shoulders, at 890 and 980 cm^{-1} (high-temperature α-$TeMo_4O_{13}$) (20). The results presented in Fig. 2 can be explained by considering that V species could partially be incorporated in the $TeMo_5O_{16}$ structure, changing the positions of the bands related to the Mo–O (bands at 913, 800, 725, and 500 cm^{-1}) and Te–O bonds (bands at 765 and 630 cm^{-1}) (18). The incorporation of Nb decreases the intensities of these bands (especially that at 905 cm^{-1}) and the appearance of new signals at 884 and 748 cm^{-1}. So, the incorporation of Nb^{5+} ions favors changes in the nature of Mo–O bonds (Fig. 2, spectra b, c, and e).

SEM–EDX Study

The morphology, crystal shape, size, and global and local chemical composition have been studied by SEM–EDX analysis (Fig. 3 and Table 2). In order to evaluate the standing of the EDX analysis, the global chemical compositions

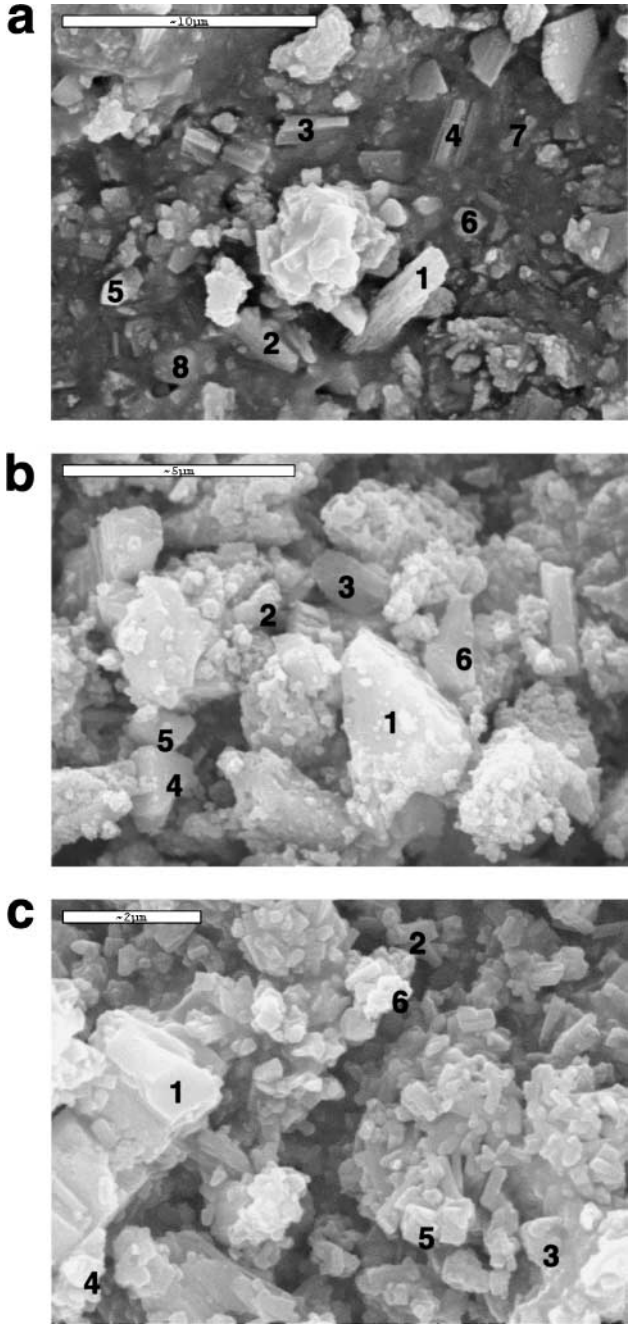

FIG. 3. SEM micrograps of MoVTeO and MoVTeNbO catalysts: (a) Cat-6; (b) Cat-7; and (c) Cat-5.

TABLE 2

EDX and XRD Results of MoVTeNbO Catalysts

Sample	EDX analysis: Particle number[a]	EDX analysis: EDX composition	XRD crystalline phases
Cat-5	1-4-6	$Mo_1V_{0.32-0.36}Te_{0.07-0.13}Nb_{0.23}$	$TeMo_5O_{16}$; Te*MO*[b];
	2-3-5	$Mo_1V_{0.40-0.50}Te_{0.24-0.37}Nb_{0.21}$	$(V_{0.07}Mo_{0.93})_5O_{14}$; $Nb_{0.09}Mo_{0.91}O_{2.80}$
Cat-6	1	$Mo_1V_{0.08}Te_{0.04}$	
	2-4-6	$Mo_1V_{0.31-0.60}Te_{0.11}$	$TeMo_5O_{16}$; Te*MO*;
	3	$Mo_1V_{0.03}Te_{0.15}$	$(V_{0.07}Mo_{0.93})_5O_{14}$
	7-8	$Mo_1V_{0.55-1.72}Te_{0.15}$	
Cat-7	1-3-4-5-6	$Mo_1V_{0.13-0.17}Te_{0.15-0.18}Nb_{0.49-0.53}$	$Mo_3Nb_2O_7$; Te*MO*
	2	$Mo_1V_{0.13}Te_{0.07-0.13}Nb_{0.40}$	

[a] Particle number in Fig. 3.
[b] Te*MO* (TeVMoO and/or TeVNbMoO phases) as indicated in Ref. 13.

obtained by this technique are in good agreement with those measured by AAS (Table 1).

The SEM image of the Nb-free sample (Cat-6) shows the presence of long rod-shape crystallites oriented in no particular direction with lengths of about 2–10 μm (Fig. 3a). This morphology is similar to that observed by Ueda and Oshihara (16) for the $Mo_6V_2Te_1O_x$, $Mo_6V_2Al_1O_x$, and $Mo_6V_2Sb_1O_x$ samples. The fact that the more important XRD reflection of Cat-6 appears at $2\theta = 22.0$ (4-Å d-spacing) could be related with the oriented crystallization of fiberlike crystals (15), aggregating to form long rod-shape crystallites. The heteroatom present in the MoVMe catalysts (Me = Al, Sb, or Te) does not affect the crystal size and a similar crystal habit is observed in all cases, which suggests that the structure in the direction of the fiber axis should be controlled by some common structural parameter, as it is the octahedral coordination of Mo(V)–O–Mo(V).

Besides the global composition, the SEM–EDX analysis evidences local inhomogeneities in the composition of crystals (Table 2), and both V-free and V-rich crystallites (with a Te/Mo ratio of 0.2 and a V/Mo ratio of 0.5, respectively) can be found. One type of crystallite can be ascribed to $TeMo_5O_{16}$, while the V-containing crystallites could be associated with the presence of MoVO mixed oxides such as $(Mo_{0.93}V_{0.07})_5O_{14}$ (the most important diffraction peak appears in the 4.09- to 4.12-Å d-spacing) and the new Te*MO* (TeVMoO and/or TeVNbMoO) crystalline phases. Furthermore, the partial incorporation of V into MoTe-containing crystals and Te into MoV-containing crystals cannot be completely ruled out. However, neither V_2O_5 nor MoO_3 were observed by either XRD or SEM/EDX techniques.

Figures 3b and 3c present the SEM micrographs of Cat-5 and Cat-7, respectively, while Table 2 shows the EDX analysis of their representative particle types. Similar SEM micrographs, containing small slabs and rods of less than 1-μm diameter with high homogeneity in their composition, have been observed in both samples. The slab and rod crystals are probably made of small fiberlike crystals aggregated along a determined axis, as for sample Cat-6. The small size of the crystals is in agreement with the higher surface areas of these samples.

XPS Study

The XPS spectra corresponding to core levels recorded for each catalyst are shown in Fig. 4. Well-resolved Mo $3d_{5/2}$, Te $3d_{5/2}$, V $2p_{3/2}$, and Nb $3d_{5/2}$ bands whose intensities depend on the chemical composition have been observed.

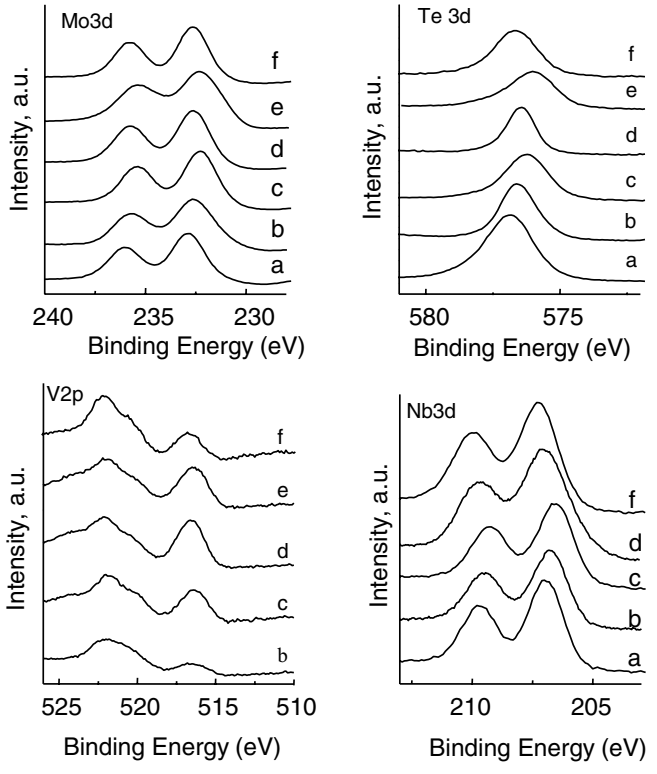

FIG. 4. Photoelectron spectra corresponding to the main transitions (Mo 3d, Te 3d, V 2p, and Nb 3d) of calcined MoVTeNb catalysts: (a) Cat-1; (b) Cat-2; (c) Cat-3; (d) Cat-5; (e) Cat-6; and (f) Cat-7.

TABLE 3

Binding Energies of Mo, V, Te, and Nb XPS for the MoVTeNbO Catalysts

Sample	Mo $3d_{5/2}$ (eV)	V $2p_{3/2}$ (eV)	Te $3d_{5/2}$ (eV)	Nb $3d_{5/2}$ (eV)
Cat-1	233.0	—	576.9	206.5
Cat-2	232.7	516.6	576.6	206.4
Cat-3	232.3	516.6	576.3	206.3
Cat-5	232.6	516.6	576.4	206.6
Cat-6	232.4	516.6	576.1	—
Cat-7	232.6	516.6	576.6	206.6

Table 1 shows the surface composition of the MoVTeNb samples while Table 3 shows the binding energies of each element obtained on samples with different chemical composition.

The Mo 3d core-level spectra of catalysts show that the binding energy of the Mo $3d_{5/2}$ changes from 232.6 to 232.3 eV, depending on the composition of catalysts (Fig. 5). The binding energy of MoO_3 is 232.5 eV, while Mo^{5+} cations are observed at 232.0 e.V. This indicates that both Mo^{6+} and Mo^{5+} are present in calcined samples, although the amount of each depends on the catalyst composition.

In the same way, the Te core-level spectra of the catalysts indicate that the binding energy of the Te $3d_{5/2}$ changes from 576.9 to 576.4 eV (Figs. 4 and 5). The BE corresponding to Te^{4+} is 576.2 eV, while H_6TeO_6 is observed at 577.3 eV (21). According to this, it can be concluded that mainly Te^{4+} cations are present in MoVTeNb catalysts, although Te^{6+} species were also observed in samples with low V contents (Fig. 5a). However, Te^0 (binding energy at 573.0 eV) was not observed.

The V $2p_{3/2}$ and the Nb $3d_{5/2}$ core-level spectra of the catalysts present binding energies at ca. 517.0 and 206.6 eV, respectively (Table 3 and Fig. 4). The intensities of both electronic levels depend on the metal content, but no significant variations of their peak widths were observed. These results suggest the presence of V^{5+} and Nb^{5+} ions.

These results are in good agreement with previous results (5, 11). In this way, the presence of Mo^{5+} cations (in the oxomolybdenum form) in distorted octahedral environments has been previously proposed from the EPR spectra in some of these catalysts (5). In addition to this, isolated V^{4+} cations were also observed. However, the amount of V^{4+} cations in our samples was very low, and V^{5+}cations appear to be the most important vanadium species, while both Mo^{6+} and Mo^{5+} cations are present in the catalysts. In the case of Te atoms, they are mainly present as Te^{4+} in MoVTeNb catalyst, although Te^{6+} cations could be present in samples with low V contents (Fig. 5).

Catalytic Results

The catalytic results obtained during the oxidation of propane on MoVTeNbO catalysts at 380°C are shown in Table 4. Acrylic acid, propene, acetic acid, and carbon oxides are the main reaction products.

In general, the study of the catalyst stability showed the same catalytic performance for 72 h. In addition, the XRD pattern of the MoVTeNbO catalysts were not modified, indicating a relative stability of these catalysts in our reaction conditions. However, their catalytic performances depend on the catalyst chemical composition.

The results shown in Table 4 suggest that V-containing catalysts are active and selective in the partial oxidation of

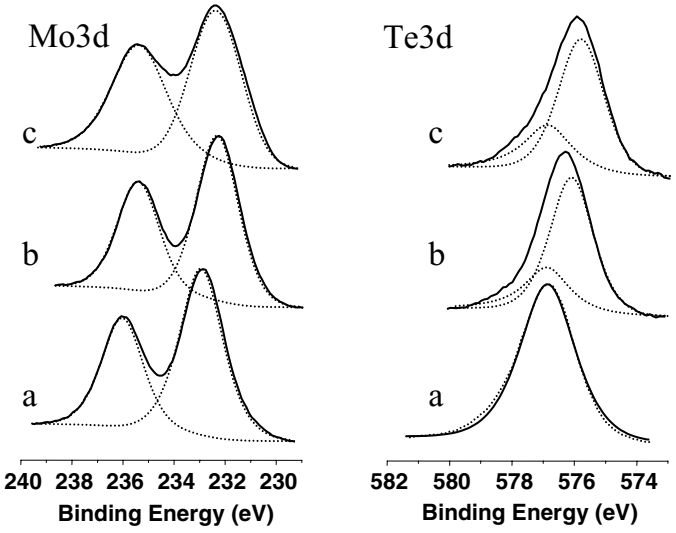

FIG. 5. Deconvolution of the Mo $3d_{5/2}$ and $3d_{3/2}$ and the Te $3d_{5/2}$ peaks for samples: Cat-1 (a); Cat-3 (b); and Cat-6 (c). (Solid line) Observed data; (broken lines) deconvoluted peaks.

TABLE 4

Catalytic Behavior of MoVTeNbO Catalysts in the Selective Oxidation of Propane at 380°C[a]

Sample	W/F[b]	Conversion (%)	STY_{AA}[c]	Selectivity (%)[e] AA	C_3H_6	AcA	CO	CO_2
Cat-1	1228	0.7	0.01	0.4	71.0	2.1	—	26.5
Cat-2	922	7.6	2.40[d]	20.2	23.3	2.0	14.9	39.6
Cat-3	205	20.5	40.5	56.3	7.1	0.7	10.8	25.1
Cat-4	205	32.1	51.6	45.9	8.4	9.2	11.6	24.9
Cat-5	205	35.2	67.1	54.3	5.0	8.8	11.1	20.8
Cat-6	1228	29.4	3.17	18.3	6.2	3.0	22.9	49.6
Cat-7	410	6.9	1.02	8.5	22.2	1.6	21.8	45.9

[a] Propane/oxygen/steam/helium molar ratio of 4/8/30/58.

[b] Contact time, W/F, in g_{cat} h $(mol_{C_3H_8})^{-1}$.

[c] Rate of formation of acrylic acid per unit mass of catalyst per unit time, STY_{AA} (space time yield), in g_{AA} kg_{cat}^{-1} h^{-1}. Calculated at propane conversions of about 30%.

[d] Space time yield of acrylic acid + propene has been considered.

[e] Selectivity to the main reaction products: acrylic acid (AA), C_3H_6, acetic acid (AcA), CO, and CO_2.

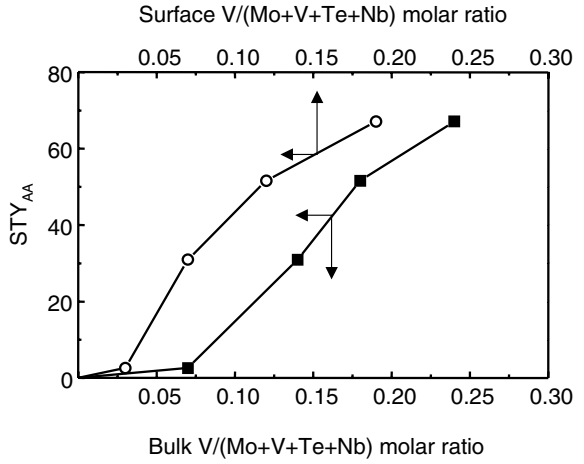

FIG. 6. Variation in the formation rate of acrylic acid with the V/(Mo + V + Te + Nb) atomic ratio in the bulk of the catalyst (determined by AAS) or with the V/(Mo + V + Te + Nb) atomic ratio on the surface of the catalyst (determined by XPS) obtained during the oxidation of propane on V-containing catalysts. Reaction conditions as in Table 5.

TABLE 5

Catalytic Behavior of MoVTeNbO Catalysts in the Selective Oxidation of Propene at 380°C[a]

Sample	W/F[b]	Conversion (%)	STY$_{AA}$[c]	Selectivity (%)[e] AA	Acrol.	AcA	CO	CO_2
Cat-1	820	5.4	3.2[d]	—	86.9	—	1.9	11.2
Cat-2	615	64.6	50.4	66.7	0.8	0	7.7	24.8
Cat-3	103	47.5	253	76.3	0.3	6.4	5.6	11.4
Cat-5	51	57.5	622	76.6	0.1	7.2	5.0	11.1
Cat-6	307	51.4	79.9	66.4	0.6	6.8	7.7	18.5
Cat-7	220	75.5	150	60.6	0.5	6.7	19.9	12.3

[a] Propene/oxygen/steam/helium molar ratio of 2/8/10/80.
[b] Contact time, W/F, in g_{cat} h $(mol_{C_3H_6})^{-1}$.
[c] Rate of formation of acrylic acid per unit mass of catalyst per unit time, STY$_{AA}$ (space time yield), in g_{AA} kg_{cat}^{-1} h^{-1}. Calculated at propene conversions of about 50%.
[d] Space time yield of acrolein has been considered.
[e] Selectivity to the main reaction products: acrylic acid (AA), acrolein (Acrol), acetic acid (AcA), CO, and CO_2.

propane to acrylic acid, although both the catalytic activity and the selectivity to acrylic acid depend on the V content. Thus, the higher the V content, the higher both the propane conversion and the selectivity to acrylic acid.

The formation rates of acrylic acid per unit mass of catalyst per unit time, STY$_{AA}$, are comparatively shown in Table 4. Space time yields of acrylic acid close to 70 g_{AA} kg_{cat}^{-1} h^{-1}, keeping selectivities to acrylic acid close to 55%, can be obtained at 380°C on these catalysts.

Figure 6 shows the variation in the formation rates of acrylic acid versus the V/(Mo + V + Te + Nb) atomic ratio in the bulk of the catalyst (determined by AAS) and on the surface of the catalyst (determined by XPS) obtained during the oxidation of propane. From these results it can be concluded that the formation of acrylic acid increases linearly with the V content of the catalyst. Since V-free MoTeNbO catalyst (Cat-1) presents a very low propane conversion (and propene was the main reaction product), V ions seem to play a key factor in the selective formation of acrylic acid from propane. Cat-3 presents a higher formation of acrylic acid than the corresponding Nb-free sample (Cat-6), and this cation appears to have also a positive effect on the selectivity to acrylic acid in V-containing catalysts. Moreover, the different catalytic activity of these samples cannot be related to the surface area of the catalyst; it must be related to the presence of Nb ions (5).

Table 5 shows the catalytic behavior of MoVTeNbO catalysts in the selective oxidation of propene. Acrylic acid, acrolein, acetic acid, and carbon oxides (CO and CO_2) were the main reaction products. In general, all the catalysts present a high selectivity to acrylic acid, although acrolein was the main reaction product on the V-free sample (Cat-1).

Figure 7 shows the variation in the formation rates of acrylic acid versus the V/(Mo + V + Te + Nb) atomic ratio in the bulk of the catalyst (determined by AAS) or on the surface of the catalyst (determined by XPS) obtained during the oxidation of propene. It can be seen that the higher the V content in the catalysts, the higher the yield to acrylic acid. In this way, a space time yield higher than 600 g_{AA} Kg_{cat}^{-1} h^{-1}, keeping selectivities to acrylic acid at about 80%, can be obtained during the oxidation of propene at 380°C.

It is known that different active sites are required for the activation of propane (V sites) and propene (Mo sites). In this way, MoTe and MoVTe catalysts are active and selective in the oxidation of propene to acrolein (22–26) and propene

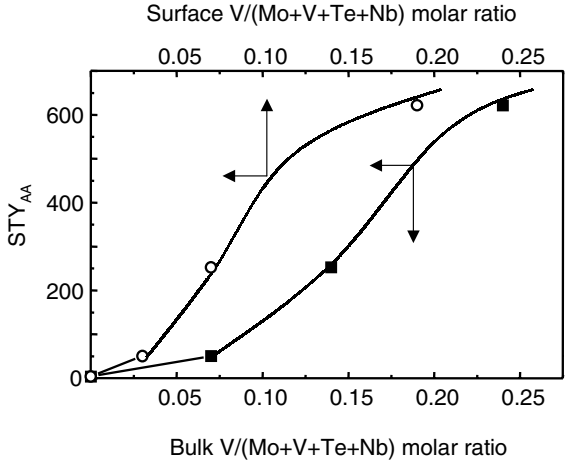

FIG. 7. Variation in the formation rates of acrylic acid with the V/(Mo + V + Te + Nb) atomic ratio in the bulk of the catalyst (determined by AAS) or with the V/(Mo + V + Te + Nb) atomic ratio on the surface of the catalyst (determined by XPS) obtained during the oxidation of propene on V-containing catalysts. Reaction conditions as in Table 5.

to acrylic acid, respectively (27, 28), and the high selectivity to acrylic acid reached on these catalysts (Table 4) could be related to the presence of V-containing crystalline phases (in addition to MoTe compounds) or to the presence of a Te*M*O (M0Mo, V and/or Nb) crystalline phases in the catalysts.

Reaction Network for Propane Oxidation

For comparative purposes, Fig. 8 shows the variation in selectivities to the main reaction products with the hydrocarbon conversion obtained during the oxidation of propene (Fig. 8a) or propane (Fig. 8b) on a MoVTeNbO (Cat-3) catalyst and on a MoVTeO (Cat-6) catalyst (Figs. 8c and 8d). Similar selectivities to acrylic acid and partial reaction products (i.e., acrolein and acrylic acid) are observed from propene oxidation for both catalysts. From the results shown in Figs. 8a and 8c, it can be concluded that acrolein and acrylic acid, in addition to CO and CO_2, are primary products during the propene oxidation on both MoVTeNbO and MoVTeO catalysts. However, the selectivity to acrylic acid increases and the selectivity to acrolein decreases with the propene conversion, which suggets that the acrylic acid could also be formed by consecutive reactions from acrolein. However, the main pathway for the acrylic acid production must be the direct conversion from propene.

From the results of propane oxidation (Figs. 8b and 8d), it can be concluded that propene, in addition to CO and CO_2, is a primary product, while acrylic acid (secondary product) is mainly formed by a consecutive reaction from propene. However, no acrolein was observed from propane. Moreover, strong differences are observed in the selectivities to partial oxidation products (propene and acrylic acid) in both catalysts; Cat-3 presents a selectivity to acrylic acid 2.5 times higher than that of Cat-6.

The initial selectivities to propene (selectivity when the propane conversion $\rightarrow$ 0) extrapolated from the results presented in Figs. 8b and 8d are close to 90 and 50% for Cat-3 and Cat-6, respectively. Since similar selectivities to acrylic acid were obtained during the oxidation of propene on these catalysts (Figs. 8a and 8c), the different catalytic performance in the oxidation of propane has to be related to the more effective activation of propane to propene (with high initial selectivity) on Cat-3. Therefore, the incorporation of Nb seems to modify the activation of propane to propene, while the same selective sites for the transformation of propene to acrylic acid are present in both catalysts.

Accordingly, the yields of acrylic acid achieved during the oxidation of propane over MoVTeNbO are close to those

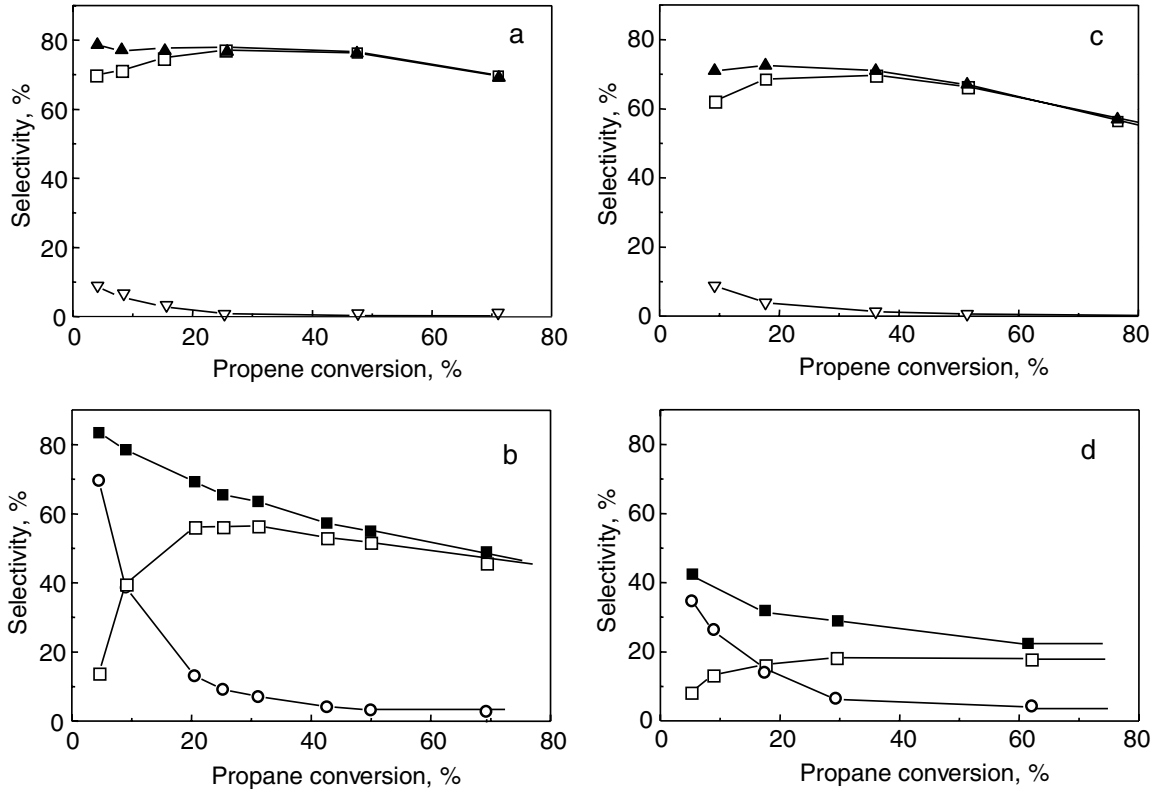

FIG. 8. Variation in the selectivities to the main partial oxidation products with the hydrocarbon conversion obtained during the oxidation of propene (a, c) or propane (b, d) at 380°C on a MoVTeNbO Cat-3 (a, b) or a MoVTeO Cat-6 (c, d), catalyst. Symbols: acrylic acid (□); propene (○); acrolein (▽); acrolein + acrylic acid (▲); and propene + acrylic acid (■).

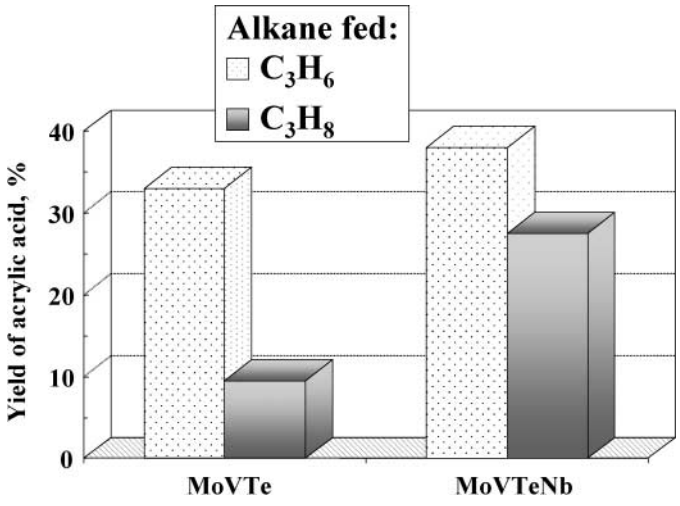

FIG. 9. Yield of acrylic acid obtained on the oxidation of propane or propene over MoVTeO (Cat-6) or MoVTeNbO (Cat-3) catalyst at 380°C. Experimental conditions as in Tables 4 and 5.

obtained from propene on MoVTeO and MoVTeNbO catalysts (Fig. 9). The yield and selectivity to acrylic acid of the catalysts presented here are higher than those reported previously for MoVTeO catalysts prepared by hydrothermal synthesis (15, 16) or for MoVTeNbO catalysts prepared by a slurry method (14, 17).

It can be concluded that there is a parallelism in the catalytic performance of these catalysts for the partial oxidation of propane and propene. A reaction network for the oxidation of propane on these catalysts, in agreement with those previously proposed (5, 14, 17), is shown in Scheme 1.

Propene is initially formed from propane on V-containing catalysts and should be consecutively transformed to acrylic acid (by an allylic mechanism), to carbon oxides (deep oxidation), and also to acrolein. Nevertheless, if this is so, the high reaction rate to acrylic acid observed during the oxidation of propene should favor a fast oxidation of acrolein to acrylic acid in the propane oxidation.

It is clear that the catalyst composition (and of course the nature of the crystalline phases) strongly influences the nature of the parallel and consecutive reactions. In this way, acetic acid was observed as a minority product during propane oxidation on these catalysts. However, acetic acid was the most important partial oxidation product dur-

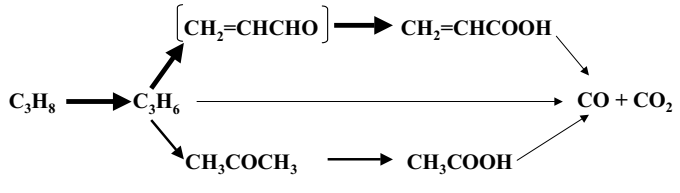

SCHEME 1. Reaction network for the selective oxidation of propane on MoVTeNbO catalysts.

ing the oxidation of propene on a MoVNbO mixed oxide catalyst (5). Hence, the formation of acetic acid can be considered a secondary reaction from the oxidation of both propene and acrylic acid.

Acetone and acetic acid are also obtained as minority products from propene over these catalysts, although they can also be formed over a MoVNb-based catalyst (5). This reaction could involve a hydration mechanism (17, 29), although their formation from C_2-hydrocarbons cannot be completely ruled out.

Nature of Active and Selective Sites

According to Scheme 1, propane is first converted into propene, which is consecutively transformed into acrylic acid. The nature of active and selective sites in these catalysts is still under discussion, although it has been proposed that at least two crystalline phases should be present on the active and selective catalysts for propane oxidation and ammoxidation. However, the nature of these crystalline phases is still unclear (1–13).

Ushikubo *et al.* (7) proposed the presence of M1 and M2 phases in their selective catalysts. The former should be effective in the oxidation of propane to propene and the latter in the oxidation of propene to acrylic acid. Recently, Aouine *et al.* (12) proposed the presence of two crystalline phases, i.e., $Te_{0.33}MO_3$ and $Te_{0.2}MO_{3.2}$ (with M = Mo, V, and Nb), in selective catalysts. These, named M1 and M2, present crystalline structures similar to those of $Sb_4Mo_{10}O_{31}$ and $Sb_2Mo_{10}O_{31}$ (or $TeMo_5O_{16}$), respectively.

In our case, more than two crystalline phases seem to be involved in our active and selective catalysts: $(Mo_{0.93}V_{0.07})_5O_{14}$, $Nb_{0.09}Mo_{0.91}O_{2.80}$, and/or $3MoO_2Nb_2O_5$ (depending on the V and Nb content). In addition, Te-containing crystalline phases can also be seen in active and selective catalysts: Mo_5TeO_{16} and the new TeMO (TeVMoO and/or TeVNbMo) crystalline phase characterized by the presence of a peak at $2\theta = 28.2$ in the XRD pattern (13). Thus, MoV-, MoNb-, and MoTe-containing crystalline phases appear to be present in our catalysts. This is in agreement with one of the possible mechanisms recently proposed by Grasselli, who indicates the presence of three moieties in selective catalysts (11).

According to our results, V appears to be a key element in the alkane activation (30, 31), although the incorporation of Nb has a possitive effect in both activity and selectivity (Tables 4 and 5 and Figs. 8 and 9). Cat-1 (V free) was inactive in propane oxidation, while the productivity to acrylic acid was dependent of the V content of catalysts (Fig. 6). Two types of V species could be proposed in our catalysts, V-containing MoO_x (or $MoNbO_x$) and V-containing Mo–Te–O phases. Moreover, the catalytic activity of V-containing MoO_x is improved after the incorporation of Nb. Cat-6 (a Nb-free catalyst) is active and relatively selective for propane oxidation but its catalytic performance is clearly

improved with the incorporation of Nb (Cat-3). The role of Nb ions, in this case, could be related to the formation of active and/or selective crystalline phases (4-Å d-spacing) (32, 33). Although $(Mo_{0.93}V_{0.07})_5O_{14}$, $3MoO_2Nb_2O_5$, and/or $Nb_{0.09}Mo_{0.91}O_{2.80}$ are observed in our catalysts, the formation of Nb-doped MoV oxide or V-doped MoNb oxide ($Mo_{5-x}(VNb)_xO_{14}$) cannot be excluded (33, 34). Thus, the selective crystalline phase for the transformation of propane to propene should be a MoVNb-containing phase or a mixture of binary phases.

The presence of a crystalline MoTe-containing phase seems to be a key factor in the selective oxidation of propene to acrolein. This reaction occurs on Te-containing MoO_3 catalysts (22–26) while the partial oxidation of propane on V-containing Te_2MoO_7 catalysts produces acrolein and acrylic acid (27, 28).

The synthesis of new Te*M*O (TeVMoO and TeVNbMoO) crystalline phases, which present XRD patterns similar to $Sb_4Mo_{10}O_{51}$ and could correspond to the phase M1 proposed by Aouine *et al.* (12), has been recently reported (13). These crystalline phases are active and selective in the propene oxidation to acrolein (TeVMoO phase) or acrylic acid (TeVNbMoO phase) but are inactive in the oxidation of propane (13). The role of V atoms in this case could be similar to that proposed for $Bi_{1-x/3}V_{1-x}Mo_xO_4$ catalysts, in which the incorporation of vanadium increases the catalytic activity for the selective oxidation of propene to acrolein (35). So, the nature of V atoms in this case should be different from those proposed in V-containing MoO_x.

According to our results, the following reaction step can be proposed (Scheme 2): (i) the activation of propane in V-sites, MoOVOMo(or Nb)-like; (ii) the oxidation of propene in Mo sites, TeOMoOTe(or V)-like; and (iii) the oxidation of acrolein to acrylic acid in Mo sites, NbOMoONb(or V) like.

The incorporation of heteroatoms in pure crystalline phases and/or the presence of heteroatoms highly dispersed on the crystalline phases should also be considered, in accordance with the EDX results (Table 2). This could be related to the formation of new ternary and/or quaternary mixed metal oxides.

This is the case of $Te_{0.33}MO_3$ (with M = MoV or MoVNb), which has been recently synthesized by our group (13). In the same way, the formation of Nb- and/or V-doped MoO_x, $Mo_{5-x}(VNb)_xO_{14}$ (33, 34), or TeM_5O_{16} (M = Mo, V, Nb) (12) should also be considered, although they have not been synthesized at this time.

In conclusion, MoVNbTe mixed metal oxides catalysts, active and selective in the partial oxidation of propane and propene to acrylic acid, have been hydrothermally prepared. Their catalytic behaviors depend on both the catalyst composition and the catalyst preparation procedure.

The catalytic behavior of these samples can be explained by the presence of different crystalline phases, i.e., $TeMo_5O_{16}$, $(Mo_{0.93}V_{0.07})_5O_{14}$, $Nb_{0.09}Mo_{0.91}O_{2.80}$, and/or $3MoO_2Nb_2O_5$, and a new Te*M*O (TeVMoO and/or TeVNbMoO) crystalline phase. However the possibility of incorporation of a heteroatom into these crystalline phases ($Mo_{5-x}(VNb)_xO_{14}$, $Te_{0.33-0.4}(VNbMo)O_x$, or $Te_2(VNbMo)_{10}O_x$) cannot be excluded.

MoVTeO and MoVTeNbO mixed oxides catalysts can selectively transform propene to acrylic acid. However, acrylic acid is only selectively obtained from propane on MoVTeNbO catalysts. Although the catalytic activity is clearly influenced by the V content of the catalyst, Nb^{5+} ions play also an important role in the catalytic behavior of these catalysts.

Furthermore, a V-containing MoTe crystalline phase could be responsible for the high selectivity to acrylic acid from propene, which could be ascribed to the formation of a V-doped $TeMo_5O_{16}$ and/or to a new Te*M*O (M = Mo, V, and Nb) crystalline phase, recently described by our group (13).

Accordingly, three or more crystalline phases are present in our active and selective catalysts. However a higher effort should be made to know clearly the nature of the active and selective sites in these multicomponent catalysts.

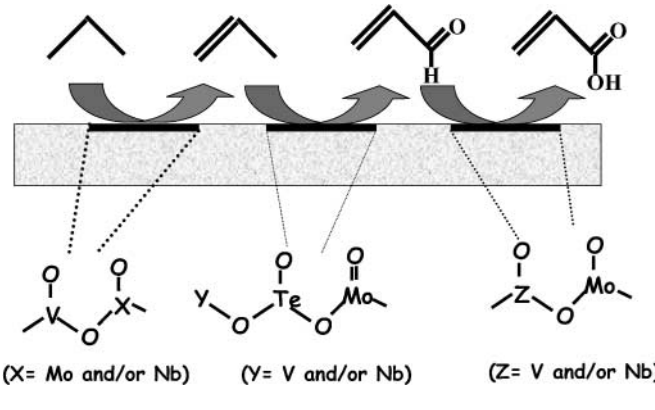

SCHEME 2. Reaction step and nature of active and selective sites in the oxidation of propane to acrylic acid on MoVTeNbO catalysts.

ACKNOWLEDGMENT

Financial support from DGICYT in Spain (Project PPQ2000/1396) is gratefully acknowledged.

REFERENCES

1. Ushikubo, T., Nakamura, H., Koyasu, Y., and Wajiki, S., U.S. Patent 5,380,933 (1995); Eur. Patent 608,838 B1 (1997).
2. Lin, M., and Linsen, M. W., Eur. Patent 962,253 (1999).
3. Komada, S., Hinago, H., Kaneta, M., and Watanabe, M., Eur. Patent 0,896,809 A1 (1999).
4. Lin, M. M., *Appl. Catal. A* **207**, 1 (2001)
5. Botella, P., López Nieto, J. M., Martinez-Arias, A., and Solsona, B., *Catal Lett.* **74**, 149 (2001).
6. Ushikubo, T., Oshima, K., Kayo, A., Umezawa, T., Kiyono, K., and Sawaki, I., Eur. Patent 0,529,853 A2 (1992).

7. Ushikubo, T., Oshima, K., Kayou, A., and Hatano, M., *Stud. Surf. Sci. Catal.* **112**, 473 (1997).
8. Ushikubo, T., *Catal. Today* **57**, 331 (2000).
9. Watanabe, H., and Koyasu, Y., *Appl. Catal. A* **194–195**, 479 (2000).
10. Asakura, K., Nakatani, K., Kubota, T., and Iwasawa, Y., *J. Catal.* **194**, 309 (2000).
11. Grasselli, R. K., *Top. Catal.* **15**, 93 (2001).
12. Aouine, M., Dubois, J. L., and Millet, J. M. M., *Chem. Commun.* 1180 (2001).
13. Botella, P., López Nieto, J. M., and Solsona, B., *Catal. Lett.* **78**, 383 (2002).
14. Luo, L., Labinger, J. A., and Davis, M. E., *J. Catal.* **200**, 222 (2001).
15. Oshihara, K., Hisano, T., and Ueda, W., *Top. Catal.* **15**, 153 (2001).
16. Ueda, W., and Oshihara, K., *Appl. Catal. A* **200**, 135 (2000).
17. Lin, M., Desai, T. B., Kaiser, F. W., and Klugherz, P. D., *Catal. Today* **61**, 223 (2000).
18. Bart, J. C. J., Cariati, F., and Sgamelloti, A., *Inorg. Chim. Acta* **36**, 105 (1979).
19. Bart, J. C. J., Petrini, G., and Giordano, N., *Z. Anorg. Allg. Chem.* **413**, 180 (1975).
20. Oganowski, W., Hanuza, J., Drulis, H., Mista, W., and Macalik, L., *Appl. Catal. A* **136**, 143 (1996).
21. Hayashi, H., Shigemoto, N., Sugiyama, S., Masaoka, N., and Saitoh, K., *Catal. Lett.* **19**, 273 (1993).
22. Grasselli, R. K., Centi, G., and Trifiró, F., *Appl. Catal. A* **57**, 149 (1990).
23. Forzatti, P., Trifiró, F., and Villa, P. L., *J. Catal.* **55**, 52 (1978).
24. Zey, S., Ruiz, B. P., and Delmon, B., *DGMK Conf.* **9705**, 165 (1997).
25. Delmon, B., Zeyss, S., Gaigneauz, E., and Ruiz, P., *Res. Chem. Intermed.* **24**, 359 (1998).
26. Andrushkevich, T. V., Boreskov, G. K., Kuznetsova, L. L., Plyasova, L. M., Tyurin, N., and Shchekochikhin, Yu., *Kinet. Catal.* **15**, 369 (1974).
27. Fedevich, E. V., Zhinevskii, V. M., Nikipanchuk, M. V., Yakubovskaya, L. F., and Golub, I .M., *Kinet. Catal.* **15**, 1140 (1974).
28. Zhinevskii, V. M., Yakubovskaya, L. F., and Tolopko, D. K., *Kinet. Catal.* **17**, 831 (1976).
29. López Nieto, J. M., Tascón, J. M. D., and Kremenic, G., *Bull. Chem. Soc. Jpn.* **61**, 1383 (1988).
30. Alboneti, S., Cavani, F., and Trifiró, F., *Catal. Rev.–Sci. Eng.* **38**, 413 (1996).
31. Blasco, T., and López Nieto, J. M., *Appl. Catal. A* **157**, 117 (1997).
32. Thorsteinson, E. M., Wilson, T. P., Young, F. G., and Kasai. P. H., *J. Catal.* **52**, 116 (1978).
33. Merzouki, M., Taouk, B., Monceaux, L., Bordes, E., and Courtine, P., *Stud. Surf. Sci. Catal.* **72**, 165 (1992).
34. Linke, D., Wolf, D., Baerns, M., Timpe, O., Schogl, R., Zeyß, S., and Dingerdisen, U., *J. Catal.* **205**, 16 (2002).
35. Ueda, W., Asakawa, H., Chen, Ch.-L., Moro-oka, Y., and Ikawa, T. J., *Catalysis* **101**, 360 (1986).